Proc. Natl. Acad. Sci. USA
Vol. 94, pp. 14450–14455, December 1997
Cell Biology

Otogelin: A glycoprotein specific to the acellular membranes of the inner ear

MARTINE COHEN-SALMON, AZIZ EL-AMRAOUI, MICHEL LEIBOVICI, AND CHRISTINE PETIT*

Unité de Génétique des Déficits Sensoriels, Centre National de la Recherche Scientifique Unité de Recherche Associée 1968, Institut Pasteur, 25 rue du Dr. Roux, 75724 Paris Cedex 15, France

Communicated by François Jacob, Institut Pasteur, Paris, France, October 23, 1997 (received for review August 27, 1997)

ABSTRACT **Efforts to identify the specific components of the mammalian inner ear have been hampered by the small number of neuroepithelial cells and the variety of supporting cells. To circumvent these difficulties, we used a PCR-based subtractive method on cDNA from 2-day-old mouse cochlea. A cDNA encoding a predicted 2910-amino acid protein related to mucin has been isolated. Several lines of evidence indicate, however, that this protein does not undergo the *O*-glycosylation characteristic to mucins. As confirmed by immunocytochemistry and biochemical experiments, this protein is specific to the inner ear. Immunohistofluorescence labeling showed that this protein is a component of all the acellular membranes of the inner ear: i.e., the tectorial membrane of the cochlea, the otoconial and accessory membranes of the utricule and saccule, the cupula of the semicircular canals, and a previously undescribed acellular material covering the otoconia of the saccule. The protein has been named otogelin with reference to its localization. A variety of nonsensory cells located underneath these membranes could be identified as synthesizing otogelin. Finally, this study revealed a maturation process of the tectorial membrane, as evidenced by the progressive organization of otogelin labeling into thick and spaced radial fiber-like structures.**

The mammalian inner ear (IE) is a complex bony and membranous structure that consists of (*i*) the cochlea, the auditory sense organ, and (*ii*) the vestibular apparatus composed of the saccule, utricle, and three semicircular canals, responsible for the sense of equilibrium. The membranous compartment of the IE is composed of a continuous series of sacs and ducts filled with endolymph and immersed in perilymph (Fig. 1*A*). These sacs and ducts contain the sensory epithelia, which consist of highly organized arrays of sensory hair cells and supporting cells. Each neuroepithelium is covered by an acellular gelatinous membrane: i.e., the tectorial membrane (TM) over the organ of Corti (Fig. 1*B*), the otoconial membranes (OMs) over the maculae of the utricule and saccule, and a voluminous gelatinous substance forming a dome-shaped cupula over the cristae of the semicircular canals; the OMs are in addition loaded with crystal-like structures, the otoconia (Fig. 1*A*). Displacement of these acellular membranes relative to the neuroepithelia, which results from the transfer of sound in the cochlea or from movements of the head in the vestibule, leads to the deflection of the sensory hair cell stereocilia bundles; this in turn opens the mechanotransduction channels (1–3).

Cytological studies have provided important insights into structural aspects of the various IE cell types (4, 5), and electrophysiological analysis has led to the elucidation of numerous mechanical properties of the structural components of the IE sensory organs (6). In contrast, the molecular components of the IE are far from being characterized. The obstacles hindering this analysis are the very small number of neuroepithelial cells and the variety of nonsensory cell types; this situation is unique to this sensory organ. To date, very few of the IE-specific proteins have been identified. In a first attempt, a protein specific to the chicken TM, β-tectorin, was purified, and antibodies raised against this protein were subsequently used to isolate the corresponding cDNA (7). Recently, degenerate oligonucleotides based on N-terminal sequence data were used to isolate the murine α- and β-tectorin cDNA (8). Such an approach, based on protein purification, is appropriate for the search of abundant proteins. An alternative strategy, consisting of the primary selection of cDNA expressed specifically in the IE, would be expected to identify more or less abundant specific components depending on the technique used. By differential screening, a cDNA encoding a rather abundant short chain collagen specific to the teleostian fish OMs has been isolated (9). To progress in the identification of the mammalian cochlear-specific components, and especially the rare ones, we used a PCR amplification-based subtractive approach on mouse cochlea cDNA (10, 11). Here, we report on the identification and the characterization of otogelin, a protein specific to the acellular membranes of the IE.

MATERIALS AND METHODS

Construction of a 2-Day-Old Mouse Cochlear Subtracted cDNA Library. Total RNA was extracted from cochlea of 2-day-old BALB/c mice, liver and brain from adult BALB/c mice, and cartilage from E20 BALB/c mice (12). Poly(A)$^+$ RNA was purified using oligo(dT) magnetic beads (Dynabeads; Dynal, New Ferry, UK). Double-stranded cDNA was synthesized by the Moloney murine leukemia virus reverse transcriptase (Superscript, GIBCO/BRL) using oligo(dT) primers. Two micrograms of each cDNA was digested by *Sau*3AI and subtracted according to the Representational Difference Analysis protocol (10, 11). Three consecutive subtractions were performed using liver cDNA to subtract the housekeeping gene products, cartilage cDNA to subtract cDNA expressed in cartilaginous tissues surrounding the IE sensory epithelium, and brain cDNA to subtract cDNA expressed in the cochlear nervous tissue.

Cloning of the Full-Length Otogelin cDNA. After the subtractions, three cDNA fragments were selected: 1A1 (position 3174–3466 bp), 0F10 (position 6995–7467 bp), and 0A3 (position 7468–7672 bp). Amplification between primers U103 (5′, 3280-TGGGACCAGAGAACCACTGTG-3′) and L244 (5′, 7243-GGCGTCGGTGCAGAATGGTGCCCTC-3′) derived from the cDNA fragments 1A1 and 0F10, respectively, was performed on double-stranded cochlear cDNA obtained

The publication costs of this article were defrayed in part by page charge payment. This article must therefore be hereby marked "*advertisement*" in accordance with 18 U.S.C. §1734 solely to indicate this fact.

© 1997 by The National Academy of Sciences 0027-8424/97/9414450-6$2.00/0
PNAS is available online at http://www.pnas.org.

Abbreviations: TM, tectorial membrane; OM, otoconial membrane; WF, von Willebrand factor; IE, inner ear; RACE, rapid amplification of cDNA ends; TGF-β2, β2-transforming growth factor.

Data deposition: The sequence reported in this paper has been deposited in the GenBank data base (accession no. U96411).

*To whom reprint requests should be addressed. e-mail: cpetit@pasteur.fr.

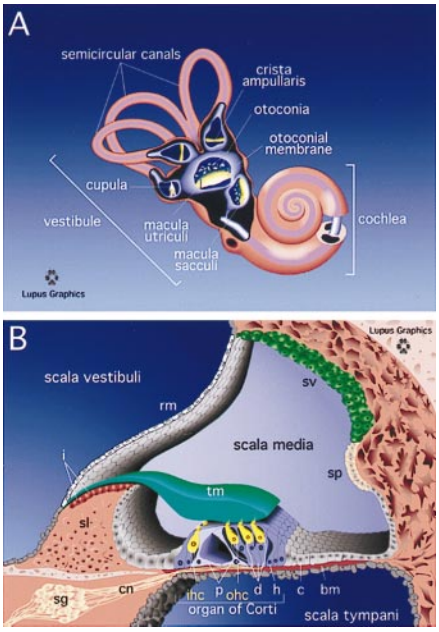

FIG. 1. (*A*) General organization of the mature inner ear. (*B*) Cross section of the cochlea. bm, basilar membrane; i, interdental cells; rm, Reissner's membrane; sv, stria vascularis; sp, spiral prominence; p, pillar cells; d, Deiter's cells; h, Hensen's cells; c, Claudius cells; ohc, outer hair cells; ihc, inner hair cells; tm, tectorial membrane; sg, spiral ganglion; cn, cochlear nerve; sl, spiral limbus.

by oligo(dT) priming, producing a band of about 4 kb, as well as smaller products of 3.2, 2.3, 2.2, and 1.5 kb. The 1.5- and 4-kb bands were cloned and sequenced, and primers in their 5′ and 3′ extremities were designed for rapid amplification of cDNA ends (RACE)-PCR amplifications on 2-day-old mouse cochlear cDNA, according to the Marathon cDNA protocol (CLONTECH), and using the Expand long template PCR *Taq* Polymerase mix (Boehringer Mannheim). 3′ extension using primers 1 (5′, 7145-TGGCAGCTTGTGAACCCCCTG-3′) and 2 (5′, 7167-CACATGCCAGGACGGGGTACTGGG-3′) on double-stranded oligo(dT)-primed cDNA gave a unique band of 3 kb that was cloned and sequenced. It contained a stop codon in the ORF as well as the entire 3′ noncoding sequence. One clone contained an insertion of 66 bp containing an alternative stop codon upstream of the one previously mentioned (see Fig. 2*A*). 5′ extension was first performed using primers 3 (5′, 3397-GGTTCTCTGGGGTCCGCATCTCAT-T-3′) and 4 (5′, 3342-CCCACCAACTGACCCTGCCACTG-AG-3′) on oligo(dT)-primed cDNA. A 1.3-kb band was obtained and sequenced. To further extend the cDNA in the 5′ direction, amplifications were then performed on 2-day-old mouse cochlear random-primed double-stranded cDNA. A first extension using primers 5 (5′, 2009-ACACCCACTGG-AGACAGGAAGTCGT-3′) and 6 (5′, 1965-GGTGCCACA-GAGGCCCACGGTGTCC-3′) gave a larger fragment of 1.6 kb long, which was cloned and sequenced. An additional extension using primers 7 (5′, 1055-TCACACCGCTCATA-CACACCCTGCA-3′) and 8 (5′, 1006- ATGGTGGGCGAG-GCAGGGAAGTAGT-3′) produced a larger band of 1 kb containing the 5′ noncoding region. Verification of the 5′ extension sequences was done by reverse transcriptase-PCR on 2-day-old mouse double-stranded cochlear cDNA using the primer 7 and U12 (5′, 12-TGGGCCAGGCTCTCTGATTG--3′). Amplifications using primers derived from this sequence did not extend the cDNA any further.

DNA Sequencing and Sequence Analysis. DNA sequencing was carried out using the PRISM Ready Reaction DyeDeoxy Terminator Cycle Sequencing Kit (Perkin–Elmer) on the ABI model 377 DNA Sequencer (Perkin–Elmer APB division).

FIG. 2. (*A*) Deduced amino acid sequence of otogelin. The signal peptide is underlined. Arrows delineate the different protein domains. WF D-type domains D1 (residues 135–498), D2 (500–870), D′ (873–971, truncated domain), D3 (972–1450), and D4 (2093–2459) share between each other and with the D domains of WF a sequence similarity of about 50%. The D3 domain contains a unique 103-residue insertion (position 1242–1394), which is shaded. The conserved residues of the multimerization site are shaded. Five WF B-type domains, B1 (2460–2492), B2 (2497–2527), B3 (2532–2563), B4 (2266–2597), B5 (2602–2632) are shown. The TSP domain (1451–2036) contains 13% threonines, 13% serines, and 15% prolines and is devoid of cysteine; CT, carboxyl-terminal end (2825–2910). The potential *N*-glycosylation sites are underlined and in bold. | indicates the additional 3′ RACE PCR alternatively spliced sequence presented at the end of the sequence. The cysteine involved in the dimerization of WF and TGF-β2 (position 2873) and the conserved glycine (position 2852) are indicated by an asterisk. The cysteines involved in the TGF-β2 knot cystine structure formation are numbered. (*B*) Schematic representation of the structure of otogelin. The thick bar indicates the predicted signal peptide.

Sequence analysis was performed using the University of Wisconsin Genetics Computer Group software (13) and the BLAST Network Service of the NCBI (14).

Production of Otogelin Fragments in *Escherichia coli*. cDNA fragments from position 3287 to 3775 and from position 4537 to 5658 were PCR-amplified using primer sets 3.*Bam*HI (5′-CGGGATCCCAGAGAACCACTGTGCAT-3′) with 4.*Hin*dIII (5′-CCCAAGCTTACTGGACAGCTGGTAGGG--3′), and 7.*Sph*I (5′-CATGCATGCGTAGCCCCACCCAC-

CTCA-3′) with 8.*Hin*dIII (5′-CCCAAGCTTTGTTCCTTG-GGGAGGCTT-3′). The PCR products were subcloned into the expression vector pQE30 (Qiagen) and overexpressed in *E. coli* according to the supplier's instructions. The histidyl-tagged (His_6-) proteins were purified as described (15).

Preparation of Rabbit Immune Sera. Male New Zealand White rabbits were primed with 300 μg of purified His_6-protein (see above) and received three additional boosts (100 μg each) at 4-week intervals.

Western Blot Analysis. Protein samples were homogenized in 150 mM NaCl, 1% Nonidet P-40, 10 mM HEPES, pH 7.4, 1 mM phenylmethylsulfonyl fluoride, 20 μg/ml leupeptin, and 20 μg/ml pepstatin, with or without 0.2 mg/ml EDTA. They were subjected to 6% SDS-PAGE using Prosieve acrylamide (Tebu). Immunoblotting with the polyclonal antiserum 7.8 (1/10,000) was performed by standard procedures (15). Non-reduced α-macroglobulin (340 kDa) and premixed high range protein marker (Boehringer Mannheim) were used for calibration.

Glycosylation Analysis. The extracts were boiled for 5 min in 1% SDS, 1% β-mercaptoethanol, diluted to a final concentration of 0.1% SDS in 20 mM sodium phosphate, pH 7.4, 1% Nonidet P-40, and digested with *Arthrobacter ureafaciens* neuraminidase (Boehringer Mannheim) (20 milliunits/ml), *Flavobacterium meningosepticum* N-glycosidase (Boehringer Mannheim) (4 units/ml), or a combination of both enzymes overnight at 37°C. The C1 inhihitor protein, which is N-glycosylated and contains sialic acids linked to O-glycosylation chains (16), was added to the protein extract as an internal control of digestion.

Multimerization Analysis. Protein samples were diluted 1:5 in 10 mM Tris, 1 mM EDTA (disodium salt) buffer, pH 8, containing 2% SDS, 8 M urea, and 0.005% bromphenol blue, incubated 15 min at 60°C, and loaded in SDS-PAGE gels.

Immunohistofluorescence. Mouse IEs were fixed by immersion in 4% paraformaldehyde (pH 7.4) for 2–5 hr at 4°C. After three PBS rinses, they were immersed in 20% sucrose-PBS for at least 12 hr at 4°C and then frozen in OCT embedding medium (Miles). Cryostat sections (7–10 μm) were stored at −80°C until use. Immunolabeling using the antiserum 3.4 (1/3000) or 7.8 (1/3000) was performed as described (15).

RESULTS

Identification of a Mouse Inner Ear cDNA Encoding a Mucin-Related Protein. Two-day-old (P2) mouse cochlear double-stranded cDNA was sequentially subtracted with mouse liver, cartilage, and brain cDNA using the representational difference analysis method (see *Materials and Methods*) (10). This stage of development, which corresponds to middle stage of the IE maturation, was chosen to identify genes implicated in the differentiation processes as well as genes encoding structural proteins. The most abundant subtracted PCR products were cloned and sequenced. Among them, three (1A1, 0F10, and 0A3) were found to encode peptides of 74, 52, and 64 amino acids, showing 71, 68, and 47% of sequence similarity, respectively, with human intestinal mucin-2 (17, 18). The possibility that these sequences belong to the same gene product was thus considered. Accordingly, they were found to hybridize to the same *Eco*RI fragment on mouse genomic DNA (data not shown). PCR amplifications with primers derived from these sequences as well as 5′ and 3′ RACE amplifications allowed us to extend the cDNA. In some of the amplification steps, more than one band was observed (see below and *Materials and Methods*). A cDNA of 10.1 kb in length was thus reconstituted. Its translation initiation site was identified by the presence of a Kozak consensus sequence CCCTGATGG at position 43, preceded by an in frame stop codon 18 bp upstream (19). This initiation codon was followed by a 8730-bp ORF and a 1281-bp 3′ untranslated region containing a single polyadenylation signal.

The predicted protein starts with a 23-amino acid sequence rich in uncharged and hydrophobic residues, characteristic of a signal peptide (Fig. 2 *A* and *B*). Its cleavage (20) would leave Thr-24 as the N-terminal amino acid of the putative 2887-residue mature protein, which has a predicted molecular mass of 313 kDa and a pI of 5.9. No evidence of either a transmembrane domain or a glycosylphosphatidylinositol anchorage sequence (21) was found in the deduced sequence, indicating that the protein is likely to be secreted. Seventeen potential N-glycosylation sites were detected (22) (Fig. 2*A*).

Analysis of the deduced amino acid sequence showed a threonine, serine, and proline-rich central region (TSP region), flanked by N- and C-terminal cysteine-rich regions, which contain motifs homologous to the B, D, and carboxyl-terminal motifs of the von Willebrand factor (WF) (23) (Fig. 2 *A* and *B*). Alignment of these motifs together and with the corresponding WF motifs showed the conservation of almost all the cysteines (data not shown). The modular organization of the present protein is reminiscent of that described for some secreted epithelial mucins (17, 18, 24, 25). However, whereas the TSP region of these proteins always contains repeated motifs (24), there was no evidence for such repetitions in the present sequence. The D domains of WF have been reported to underlie the multimerization of the protein (26). In particular, the CGLC motif of the WF D1 and D2 repeats, which corresponds to the consensus sequence of the catalytic site of several disulfide isomerases, has been demonstrated to catalyze the oligomerization of the WF (27). However, only the last three amino acids of this motif (GLC) are present in the four WF D domains of the present protein sequence, arguing against a WF-type oligomerization (Fig. 2*A*). No particular function has yet been assigned to the B repeats in WF. The carboxyl-terminal end of the present protein shares several characteristics with the carboxyl-terminal regions of proteins such as WF, some secreted epithelial mucins, the Norrie disease protein, the β2-transforming growth factor (TGF-β2), the nerve growth factor, and other related neurotrophins (reviewed in ref. 28). It contains six cysteines that have been demonstrated to form three intramolecular disulfide bridges in nerve growth factor, TGF-β2, and Norrie disease protein, resulting in the formation of a cystine knot structure required for the subsequent homodimerization of these proteins (29, 30) (Fig. 2*A*). The cysteine implicated in the formation of homodimers in TGF-β2 and in WF is also conserved in the present sequence (31, 32), as is a glycine that has been shown to be structurally important in the cystine knot domain (Fig. 2*A*). Finally, the predicted secondary structure of this domain shows β-strands and loop regions similar to those observed in nerve growth factor and TGF-β2 (data not shown).

As mentioned above, several additional PCR products were obtained during the reconstitution of the cDNA. Of the two sequenced, one was predicted to encode a polypeptide in which part of the WF D3 domain (position 1141–1429) and part of the TSP and WF D4 domains (position 1740–2371) were absent; the other one was found to contain an insertion of 66 bp in the sequence encoding the WF B5 domain (position 2617) (Fig. 2*A*). The first seven amino acid residues encoded by this sequence were identical to the residues 2618–2624 but were followed by a stop codon. These data suggested the existence of various isoforms of the protein resulting from alternative splicing.

Otogelin, an N-Glycosylated Protein Specific of the Inner Ear. Because no signal was detected using Northern blot analysis, the expression of the gene was first analyzed by *in situ* hybridization on parasagittal sections of whole mouse embryos at postnatal day 2 (P2) using the 1A1, 0F10, and 0A3 fragments of the cDNA. The expression was found to be restricted to the cochlea and vestibular organ (not shown). This result was further confirmed by reverse transcriptase-RCR performed on total RNA extracted from various tissues (data not shown).

Rabbit immune sera were raised against recombinant protein fragments containing either the WF D3 domain (antiserum 3.4) or the TSP region (antiserum 7.8) (see *Materials and Methods*). Although both antisera detected the protein on tissue sections, only antiserum 7.8 detected the protein on Western blot. Protein extracts from the IE, eye, brain, kidney, spleen, and liver of 15-day-old mice, as well as from two mucin-rich tissues (i.e., intestine and lung), were analyzed (Fig. 3*A*). Bands were only detected in the IE. Under reducing conditions, two major bands were observed: i.e., one at about 340 kDa and a diffuse band ranging from 240 to 270 kDa, as well as four minor bands at about 170, 150, 115, and 110 kDa. The corresponding protein was named otogelin with reference to its tissue specificity and location (see below).

The glycosylation of otogelin was investigated by digesting mouse IE protein extracts with neuraminidase or N-glycosidase, either alone or in combination (see *Materials and Methods*) (Fig. 3*B*). Neuraminidase did not cause any shift of the electrophoretic mobility of the bands. After treatment with N-glycosidase, however, the mobility of the three bands increased: the 340-kDa band shifted to approximately 320 kDa, and the diffuse band ranging from 240 to 270 kDa shifted to 230–260 kDa. The same result was obtained when the two enzymes were combined.

Finally, the ability of the protein to form covalent oligomers was tested by studying the migration of urea/SDS-denatured P15 cochlear extracts under nonreducing conditions (Fig. 3*C*). A mobility shift was observed only for the two higher bands, which appeared to migrate faster, thus indicating the presence of intramolecular disulfide bridges. In addition, two new bands, one at about 650 kDa and a diffuse band at around 450 kDa, were observed, which could correspond to the homodimerization of the two major bands detected under reducing conditions. Such dimerization of the protein would be consistent with the presence of the cystine knot motif in the carboxyl-terminal part of the deduced amino acid sequence (see above).

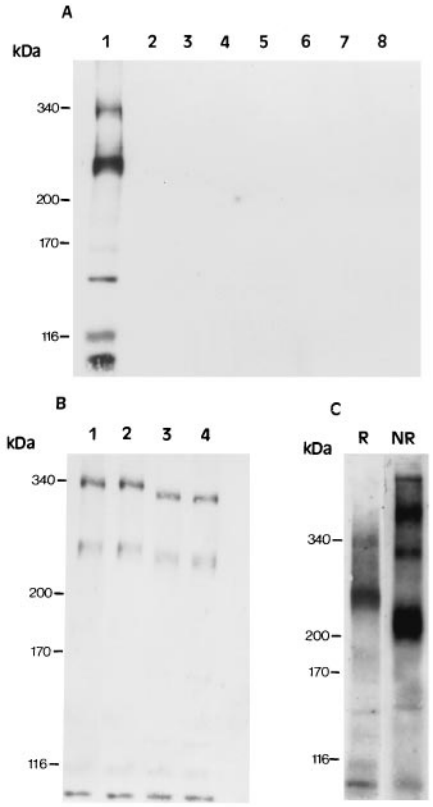

FIG. 3. Western blot analysis of otogelin using the 7.8 antiserum. Molecular mass standards (in kDa) are indicated on the left. (*A*) Tissue distribution of otogelin in the P15 mouse: inner ear (1), eye (2), brain (3), liver (4), intestine (5), kidney (6), spleen (7), and lung (8). (*B*) Deglycosylation assays of P2 mouse inner ear extracts: control buffer (1), neuraminidase (2), *N*-glycosidase (3), both enzymes (4). Note that the concentration of the diffuse 240–270-kDa band and the 170- and 150-kDa bands were weaker compared with 15-day-old extracts. (*C*) P15 mouse cochlear extracts in denaturing reducing (R) and nonreducing (NR) conditions (see *Materials and Methods*).

Expression Pattern of Otogelin in the Inner Ear. The distribution of otogelin in the mouse IE was studied at postnatal stages (P) by immunohistofluorescence using either the 7.8 or the 3.4 immune serum (see *Materials and Methods*); both gave the same results. In the cochlea at P0 (Fig. 4*A*), the pseudostratified cells of the greater epithelial ridge, as well as all the supporting cells of the neuroepithelium comprising the Deiter's cells, the Hensen's cells, and the pillar cells, were labeled. The Claudius cells, which form the most external part of the floor, were also immunoreactive. Otogelin was also detected in the epithelial cells of the Reissner's membrane as well as in a small set of cells comprising the spiral prominence. The cells of the stria vascularis were not labeled. Finally, both the minor TM covering the neuroepithelium from Hensen's cells to the outer hair cells, and the major TM covering the spiral limbus and the greater epithelial ridge, were intensely labeled. From this stage, the cellular expression of otogelin decreased until P6, where the immunostaining was present mainly in the TM (Fig. 5*B*). However, at P15, a faint labeling was detected within the interdental cells (Fig. 4*B*), located just underneath the limbal part of the TM.

In the vestibular apparatus, otogelin immunolabeling was stronger than in the cochlea. At birth (Fig. 4*C*), an intense

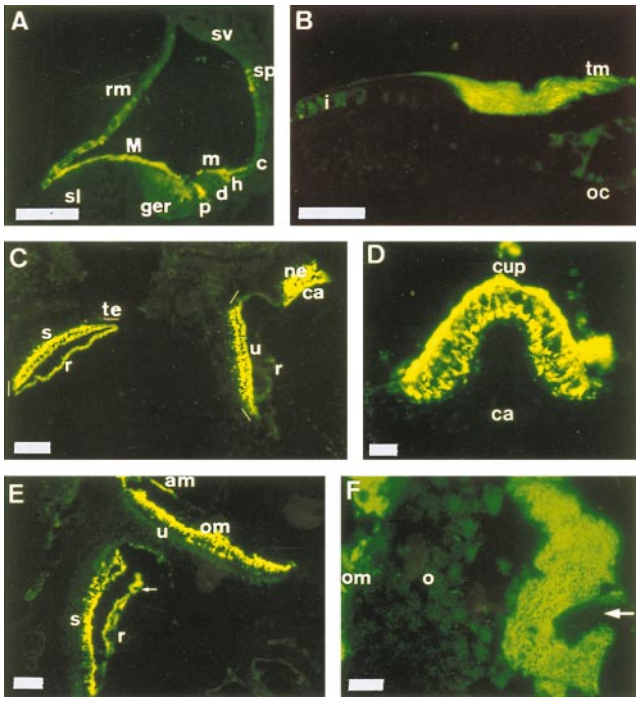

FIG. 4. Otogelin in the inner ear by immunohistofluorescence using the 7.8 antiserum. (*A*) Cochlea at P0. (*B*) Cochlea at P15. (*C*) Vestibule at P0. (*D*) Anterior crista ampullaris at P4. (*E*) Saccule and utricle at P20. (*F*) Saccule at P20 (laser confocal microscopy). The arrowhead in *E* and *F* indicates the staining covering the otoconia (○). ger, greater epithelial ridge; M, major tectorial membrane; m, minor tectorial membrane; s, saccule; u, utricle; ca, crista ampullaris; te, transitory epithelium; ne, neuroepithelium; r, roof; cup, cupula; ca, crista ampullaris; om, otoconial membrane; am, accessory membrane. (*C*) The OMs and the cupula were lost during tissue preparation. Other abbreviations as before. Scale bars: 60 μm (*A*), 50 μm (*B*), 100 μm (*C–E*), 10 μm (*F*).

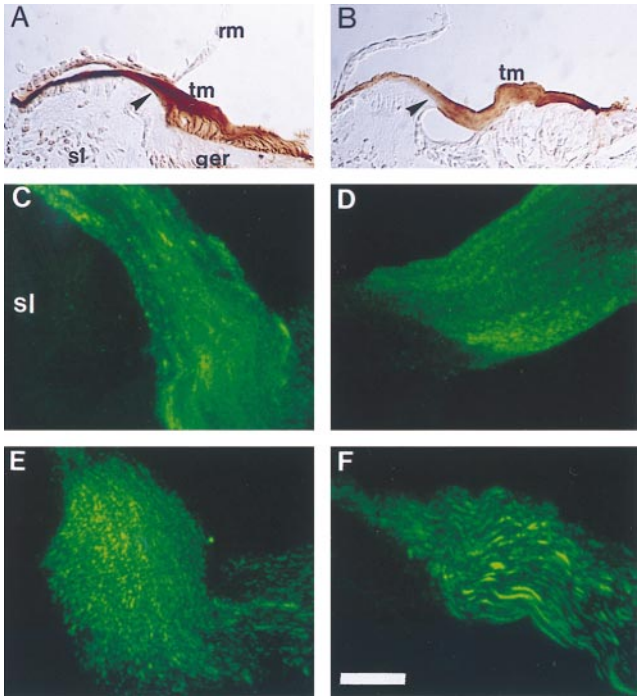

FIG. 5. Otogelin in the tectorial membrane. Immunoperoxidase labeling at P4 (*A*) and P6 (*B*) with the 7.8 antiserum. Immunohistofluorescence using the 7.8 antiserum and laser confocal microscopy of the outer edge of the spiral limbus area (arrowhead in *A* and *B*) at P4, (*C*), P6 (*D*), P8 (*E*), and P20 (*F*). The tectorial membrane has the same orientation in all of the figures (*A–F*). Abbreviations as before. Scale bar: 100 μm (*A*, *B*), 10 μm (*C–F*).

staining was observed in all the supporting cells of the saccular and utricular maculae as well as in those of the cristae ampullares of the three semicircular canals. The OMs of the saccule and the utricle, and the cupula in the cristae ampullares were also labeled. In the neuroepithelia of the utricle and the saccule, the labeling extended beyond the macula to the surrounding transitory epithelium. Otogelin was also detected in the epithelial cells of the roof of the saccule but not in the roof of the utricle and cristae ampullares. At P20, most of the otogelin immunostaining was detected in the cupula, the OMs, and the accessory membranes that surround the otoconia laterally in the saccule and the utricle (Fig. 4 *D* and *E*). In addition, staining of a previously undescribed acellular material covering the otoconia of the saccule was observed (Fig. 4 *E* and *F*).

Otogelin in the Tectorial Membrane. Otogelin immunostaining in the TM was analyzed both by immunoperoxidase histochemistry and by laser confocal microscopy (Fig. 5). At P4, strongly immunostained strands were observed in the region of the major TM over the greater epithelial ridge, running vertically along its basal part in close contact with the cells underneath; in contrast, the staining of the upper part of the TMs seemed homogeneous (Fig. 5*A*). At P6, the major and minor TMs have fused, forming a single TM, which was more homogeneously stained than at P4 (Fig. 5*B*). No more vertical strands were observed in contact with the greater epithelial ridge, which had receded to form the inner sulcus (Fig. 5*B*). At P8, within the TM, immunostained spots, partially aligned and oriented radially toward the tip of the TM, were observed (Fig. 5*E*). From P15 onward, the immunolabeling of the TM exclusively consisted of thick and strongly labeled strands extending radially (Fig. 5*F*).

DISCUSSION

Using a PCR-based subtractive method, we have identified a murine glycoprotein, otogelin, which is specifically expressed in developing and mature IE.

The overall primary structure of otogelin is reminiscent of that of epithelial-secreted mucins as it comprises a central TSP region flanked by WF-like cysteine-rich domains (Fig. 2*B*; reviewed in ref. 24). However, several lines of evidence argue against mucin-like *O*-glycosylation (33) of the otogelin TSP region. First, the apparent molecular mass of the highest band observed by Western blot analysis in reducing conditions upon *N*-glycosidase treatment corresponds to the molecular mass predicted from the 2910-amino acid deduced sequence of the protein. Second, neuraminidase treatment of IE protein extracts did not affect the electrophoretic mobility of otogelin, whereas this enzymatic treatment usually slows down the migration of the mucins due to the loss of the negatively charged sialic acids linked to the *O*-glycosylated chains (34). Third, the antiserum raised against the TSP region of otogelin produced in a bacterial system detected both the intracellular and the secreted forms of the protein upon immunohistofluorescence analysis, whereas mature mucins are usually not detected by antibodies elicited in the same conditions, due to the masking of the corresponding epitopes by the *O*-glycosylation (35). In addition, the TSP region of otogelin does not contain the repeated motifs that are present in every epithelial mucin. Therefore, it is unlikely that otogelin corresponds to a mucin.

Several explanations could account for the complex pattern of bands observed by Western blot analysis. These bands may (*i*) correspond to proteins encoded by different genes specifically expressed in the cochlea; (*ii*) result from proteolytic cleavage of otin, which would take place *in vivo* as the same pattern was observed when protein extracts were prepared in the presence of EDTA (data not shown); (*iii*) result from alternative splicing of a single transcript. Whereas the second possibility cannot be excluded, we favor the last hypothesis. Indeed, no genes closely related to *otogelin* could be detected by Southern blot analysis of mouse genomic DNA hybridized with various fragments of the otogelin cDNA at low stringency (data not shown). Moreover, the results obtained provide evidence for the existence of alternatively spliced transcripts.

During the last 15 years, much work has been devoted to defining the contribution of neuroepithelial supporting cells in the secretion of acellular membrane components. Whereas most of these studies have concentrated on the formation of the TM (reviewed in ref. 36), the present study enabled us to get an insight into the contribution of the various cell populations to the synthesis of a single component of all the acellular membranes of the IE. In the cochlea and the vestibular apparatus, all the neuroepithelial supporting cells were labeled, which is consistent with the staining of the above TM, OMs, and cupulae in their entirety, and from their appearance at E15 (data not shown). Similarly, expression of otogelin in the transitory epithelium of the saccule and utricle correlated with the formation of the accessory membranes, which constitute the lateral wall of the OMs. Otogelin seemed also to be transiently synthesized in the roof of the saccule but not of the utricle. As this expression decreased, an immunostained extracellular material covering the otoconia of the saccule was observed. Surprisingly, this structure, which might play a role in limiting the movements of the otoconia, has not previously been reported in morphological studies of the saccule. Based on the present findings, it is tempting to propose that this acellular material is secreted by the roof of the saccule. In addition, otogelin synthesized by the epithelial cells of Reissner's membrane in the cochlea at P0 might also contribute to the TM. Finally, the possible renewal of the components of the mature TM during adult life has long been debated. Interdental cells would be expected to be involved as they are the only cells that maintain contact with the TM in the adult. Arguing in favor of this renewal, interdental cells were the only cells where otogelin could be detected after complete maturation of the TM.

During the period of secretion of otogelin by the supporting cells located underneath the TM, labeled vertical strands in the basal part of the TM contacting the neuroepithelium were observed. These strands disappeared at P6, which is at the time when no more otogelin synthesis was detectable in these cells, being replaced by a homogeneous labeling of the TM. From this stage to P15, progressive changes in the distribution of the protein were observed, ending up in the immunodetection of radial and well separated fibers throughout the TM. Similar fiber-like structures were observed in the OMs and the cupula (data not shown). Western blot analysis, performed at a stage when otogelin labeling appears as fiber-like structures, showed that the bulk of the protein is not involved in disulfide-linked polymers. This therefore indicates that the observed fiber-like structures could result from a noncovalent interaction of otogelin monomers either between themselves or, more likely, to a fiber network. Such fibrillar structures have already been described in the TM by ultrastructural studies (37, 38). These consist of straight unbranched thick fibrils, 10 nm in diameter, referred to as type A fibrils, organized in bundles that are separated by a matrix containing thinner fibrils, 7 nm in diameter, referred to as type B fibrils (37). The type A fibers contain type II collagen fibrils, cross-linked with type IX collagen (39, 40). These fibrils have been proposed to be responsible for the rigidity of several connective tissues (41) and are therefore thought to play a crucial role in the rigidity of the TM. The type B fibrils have been shown to be composed of type V collagen and unknown glycoproteins (39, 42). Otogelin fiber-like immunolabeling is not likely to correspond to the type B fibrils, which are diffuse and highly concentrated in some superficial regions of the TM (37), but it could correspond to the type A fibrils, which are radially distributed throughout the TM (39). Recently, two other molecules of the TM have been isolated in mouse, the α- and β-tectorins (8). These proteins contain, in their carboxyl-terminal region, a domain described in some proteins of the zona pellucida of the ovocyte (43). In addition, α-tectorin has WF D domains containing the oligomerization consensus site CGLC (27), as well as a domain homologous to the entactin/nidogen protein (44). Based on these homologies, these proteins have been proposed to form fibrillar structures in the TM. *In situ* hybridization studies suggest that these two proteins, like otogelin, are also present in the utricle and saccule. However, in the vestibular apparatus, their distribution seems to be different to that of otogelin, with α-tectorin being mainly expressed in the transitory epithelium as well as in the roof of the saccule and utricle, and β-tectorin, being present in a restricted region of the maculae called the striola. Compared with the tectorins, otogelin seems also to be less abundant in the TM, as none of the otogelin major bands has been observed in the previous Coomassie-stained gels of the mouse TM proteins (45, 46).

Future work is therefore needed to elucidate how otogelin and the other components of the TM interact to ensure the structural stabilization and the tensile strength of this membrane, which play a crucial role in the auditory mechanotransduction process.

We thank J.-P. Hardelin, E. Verpy, V. Kalatzis, and E. Heard for critical reading of the manuscript, P. Küssel for the drawing of Fig. 1, F. Crozet for technical help, and R. Hellio for help in confocal microscopy. M.C.S. is supported by the Association Française contre les Myopathies (AFM). This work is supported by AFM Grant 4922, Commission of the European Community Grant PL951324, and Centre National de la Recherche Scientifique (CNRS) Grant 97N60/0593.

1. Hudspeth, A. J. (1989) *Nature (London)* **341,** 397–404.
2. Hudspeth, A. J. & Gillepsie, P. G. (1994) *Neuron* **12,** 1–9.
3. Denk, W., Holt, J. R., Sheperd, G. M. G. & Corey, D. P. (1995) *Neuron* **15,** 1311–1321.
4. Lim, D. L. & Anniko, M. (1985) *Acta Otolaryngol. Suppl.* **42,** 1–69.
5. Tilney, L. G., Tilney, M. S., Saunders, J. S. & DeRosier, D. J. (1986) *J. Cell Biol.* **106,** 355–365.
6. Dallos, P. & Evans, B. N. (1995) *Science* **267,** 2006–2009.
7. Killick, R., Legan, P. K., Malenczak, C. & Richardson, G. P. (1995) *J. Cell Biol.* **129,** 535–547.
8. Legan, K. P., Rau, A., Keen, J. N. & Richardson, G. P. (1997) *J. Biol. Chem.* **272,** 8791–8801.
9. Davis, J. G., Oberholtzer, J. C., Burns, F. R. & Greene, M. I. (1995) *Science* **267,** 1031–1034.
10. Lisitsyn, N., Lisitsyn, N. & Wigler, M. (1993) *Science* **259,** 946–951.
11. Hubank, M. & Schatz, D. G. (1994) *Nucleic Acids Res.* **22,** 5640–5648.
12. Chomczynski, P. & Sacchi, N. (1987) *Anal. Biochem.* **162,** 156–159.
13. Devereaux, J., Haeberli, P. & Smities, O. (1984) *Nucleic Acids Res.* **12,** 387–395.
14. Altschul, S. F., Gish, W., Miller, W. & Myers, E. W. (1990) *J. Mol. Biol.* **215,** 403–410.
15. El-Amraoui, A., Sahly, I., Picaud, S., Sahel, J., Abitbol, M. & Petit, C. (1996) *Hum. Mol. Genet.* **5,** 1171–1178.
16. Bock, S. C., Skriver, K., Nielsen, E., Thogersen, H.-C., Wiman, B., Donaldson, V. H., Eddy, R. L., Marrinan, J., Radziejewska, E., Huber, R., Shows, T. B. & Magnusson, S. (1986) *Biochemistry* **25,** 4292–4301.
17. Gum, J. R., Hicks, J. W., Toribara, N. W., Rothe, E.-M., Lagace, R. E. & Kim, Y. S. (1992) *J. Biol. Chem.* **267,** 21375–21383.
18. Gum, J. R., Hicks, J. W., Toribara, N. W., Siddiki, B. & Kim, Y. S. (1994) *J. Biol. Chem.* **269,** 2440–2446.
19. Kozak, M. (1986) *Cell* **44,** 283–292.
20. Von Heijne, G. (1986) *Nucleic Acids Res.* **14,** 4683–4690.
21. Englund, P. T. (1993) *Annu. Rev. Biochem.* **62**, 121–138.
22. Bause, E. (1983) *Biochem. J.* **209,** 331–336.
23. Verweij, C. L., Diergaarde, P. J., Hart, M. & Pannekoek, H. (1986) *EMBO J.* **5,** 1839–1847.
24. Gendler, S. J. & Spicer, A. P. (1995) *Annu. Rev. Physiol.* **57,** 607–634.
25. Joba, W. & Hoffmann, W. (1997) *J. Biol. Chem.* **272,** 1805–1810.
26. Voorberg, J., Fontijn, R., vanMourik, J. A. & Pannekoek, H. (1990) *EMBO J.* **9,** 797–803.
27. Mayadas, T. N. & Wagner, D. D. (1992) *Proc. Natl. Acad. Sci. USA* **89,** 3531–3535.
28. Bork, P. (1993) *FEBS Lett.* **327,** 125–130.
29. McDonald, N. Q. & Hendrickso, W. A. (1993) *Cell* **73,** 421–424.
30. Meitinger, T., Meindl, A., Bork, P., Rost, B., Sander, C., Haasemann, M. & Murken, J. (1993) *Nat. Genet.* **5,** 376–380.
31. Voorberg, J., Fontijn, R., Calafat, J., Janssen, H., van Mourik, J. A. & Pannekoek, H. (1991) *J. Cell Biol.* **113,** 195–205.
32. Schneppenheim, R., Brassard, J., Krey, S., Budde, U., Kunicki, T. J., Holmberg, L., Ware, J. & Ruggeri, Z. M. (1996) *Proc. Natl. Acad. Sci. USA* **93,** 3581–3586.
33. Bansil, R., Stanley, E. & LaMont, J. T. (1995) *Annu. Rev. Physiol.* **57,** 635–657.
34. McCool, D. J., Forstner, J. F. & Forstner, G. (1994) *Biochem. J.* **302,** 111–118.
35. vanKlinken, J.-W. B., Oussoren, E., Weenink, J.-J., Strous, G. J., Büller, H. A., Dekker, J. & Einerhand, A. W. C. (1996) *Glycoconj. J.* **13,** 757–768.
36. Lim, D. & Rueda, J. (1992) in *Development of the Auditory and Vestibular System 2*, ed. Romand, R. (Elsevier, Amsterdam), pp. 33–58.
37. Kronester-Frei, A. (1978) *Cell Tissue Res.* **193,** 11–23.
38. Hasko, J. A. & Richardson, G. P. (1988) *Hearing Res.* **35,** 21–38.
39. Slepecky, N. B., Savage, J. E., Cerafatti, L. K. & Yoo, T. J. (1992) *Cell Tissue Res.* **267,** 413–418.
40. Slepecky, N. B., Savage, J. E. & Yoo, T. J. (1992b) *Acta Otolaryngol.* **112,** 611–617.
41. van der Rest, M. & Mayne, R. (1988) *J. Biol. Chem.* **263,** 1615–1618.
42. Richardson, G. P., Russell, I. J., Duance, V. C. & Bailey, A. J. (1987) *Hearing Res.* **25,** 45–60.
43. Bork, P. & Sander, C. (1992) *FEBS Lett.* **300,** 237–240.
44. Yurchenco, P. D. & Schittny, J. C. (1990) *FASEB J.* **4,** 1577–1590.
45. Khalkhali-Ellis, Z., Hemming, F. W. & Steel, K. P. (1987) *Hearing Res.* **25,** 185–191.
46. Killick, R. & Richardson, G. P. (1997) *Hearing Res.* **103,** 131–141.